www.ietdl.org

Published in IET Wireless Sensor System
Received on 23rd February 2011
Revised on 14th May 2011
doi: 10.1049/iet-wss.2011.0033

ISSN 2043-6386

Probability of early detection of ultra-wideband positioning sensor networks

T. Hazim[1] *G.K. Karagiannidis*[1] *T.A. Tsiftsis*[2]

[1]Department of Electrical Engineering, Aristotle University of Thessaloniki, 54124 Thessaloniki, Greece
[2]Department of Electrical Engineering, Technological Educational Institute (TEI) of Lamia, 35100 Lamia, Greece
E-mail: tsiftsis@teilam.gr

Abstract: Ultra-wideband (UWB) sensor networks can be efficiently applied to collect data through sensors deployed for preserving environment and rescuing lives. The high-precision positioning capabilities of UWB technology, based on its operation of ultra-short data bearing pulses, can be a reliable solution for such applications. Most of the UWB positioning techniques are based on time-of-arrival of the first path which can be effectively estimated when the probability of early detection (PoED) is accurately evaluated. In this study, we study the PoED of UWB positioning sensor networks subject to narrowband interference modelled with Nakagami-m distribution. We derive novel closed-form approximate expressions which are simpler and have remarkable accuracy compared to the previously published semi-infinite series expressions. Furthermore, to simplify our approach, we present tight lower and upper closed-form bounds for the PoED. Numerical results and simulations are performed to validate the analytical derivations.

1 Introduction

Ultra-wideband (UWB) communication has some very attractive features over traditional wireless transmission technologies such as applications for networking, imaging, radar, emergency communications and also efficient ranging-positioning capabilities that is the UWB positioning systems. All these benefits arisen by the inherent technology of UWB where ultra-short data bearing pulses are transmitted. One of the major benefits of UWB technology is its capability of accurate position estimation in highly cluttered environments [1–4]. UWB positioning systems offer high accuracy compared to the traditional Global Positioning System owing to its efficiency in cluttered environments and its high temporal resolution and multipath immunity [5–7].

Sensor networks are usually asynchronous wireless networks where no infrastructure is required and with nodes consisting of handheld devices carried by people or wireless sensors. Nodes in such networks discover each other automatically when the network is deployed and communicate directly with each other with no user intervention and thus exploit the advantages of autonomous behaviour, self-organisation abilities and adaptability to changing environment [3]. In Fig. 1, we present a possible scenario where a number of sensors form a wireless UWB sensor network. This sensor network spans over a forest tree and is capable of preventing unwanted situations such as a fire disaster. Each UWB sensor can send information data via the network to the monitoring server and/or notify any UWB user in a short-to-medium range. A similar application was presented in [8–10] where the deployment strategy for sensors was investigated.

There are many techniques to estimate the positioning of a target node of which the time-based approach positioning technique is the most efficient owing to its accuracy in measurements. The estimation of the range between the target and the node is based on the estimation of the time-of-arrival (ToA) of the signal at the receiver and specifically the arrival of the first path [11–13]. The ToA estimation in UWB receivers can be evaluated via a simple technique based on the utilisation of energy detectors (EDs) and specifically on the probability of detecting the first path, that is the probability of early detection (PoED). The low-complexity circuitry ED, which is operated at sub-Nyquist sampling rates, detects the first signal path by comparing its output with a predefined threshold [14]. In several previous published papers the estimation of ToA of UWB positioning systems under narrowband (NBI) and wideband interference (WBI) has been investigated. In the important works of Dardari *et al.* in [11, 12], the authors have evaluated the performance of the UWB positioning systems in the presence of NBI and WBI. However, in both works the PoED is presented as semi-infinite nested sums.

In this paper, we evaluate the PoED of the first path when the UWB positioning sensor network is experienced NBI subjected to Nakagami-m fading. Specifically, we derive an accurate approximate closed-form expression as a finite sum of the confluent hypergeometric function $U(\cdot;\cdot;\cdot)$. Furthermore, to simplify the above expressions, we present tight upper and lower bounds on the PoED of the first path. The bounds are obtained in a unified closed form as a finite sum in terms of complementary error function $\mathrm{erfc}(\cdot)$ and confluent hypergeometric function ${}_1F_1(\cdot;\cdot;\cdot)$. The derived analytical results are validated by

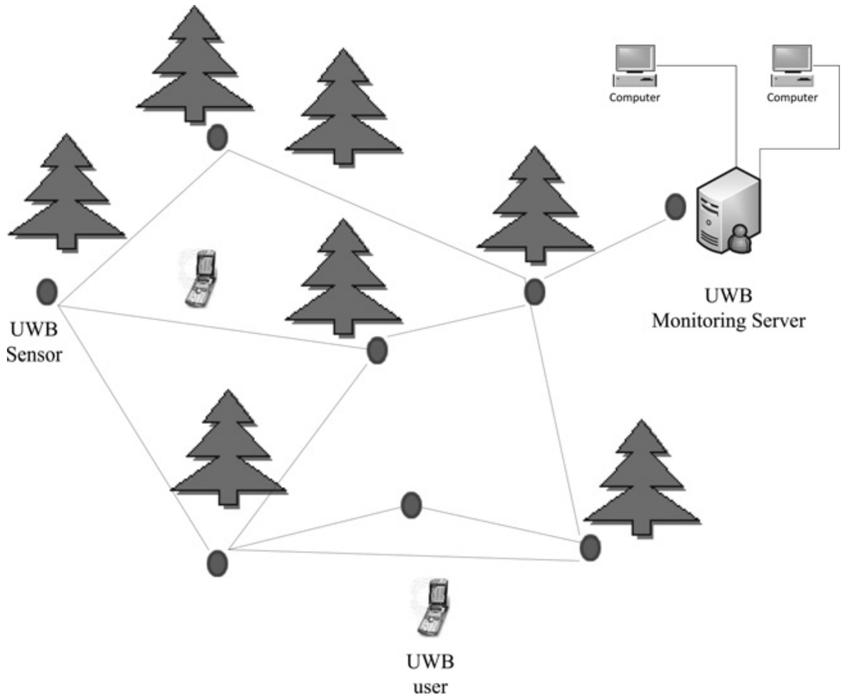

Fig. 1 *UWB sensor network for environmental applications*

simulations that verify the accuracy of the analytical expressions.

The novelty and technical contribution of this paper is three-fold:

1. Theoretical analytical results of the application of UWB technology in outdoor environments are presented. Specifically, we efficiently estimate the position of a node in a wireless sensor network that is useful for emergency communications. The analysis can be an efficient tool for rescue teams to accurately locate where people involved in accidents and thus rescuing lives.
2. Simple closed-form expressions for the PoED of the first path of UWB signals which is absolutely necessary for estimating the ToA of the first path are derived. The first path, in most cases, is not the strongest signal making the estimation of both the PoED and ToA an interesting issue.
3. Lower and upper tight bounds on the PoED are also derived which not only simplify the above expressions but also give to the researchers the necessary tools to efficiently calculate the lower and upper limits of the PoED.

This paper is organised as follows: Section 2 provides the system and channel model of the UWB positioning system under consideration. Section 3 describes the proposed analytical methodology for the derivation of the PoED. Tight lower and upper bounds are presented in Section 4. The derived PoED analytical results are compared with Monte Carlo simulations in Section 5. Finally, some concluding remarks are given in Section 6.

2 System and channel model

We consider a non-coherent estimation system where an ED is used, which it is capable of estimating the ToA of the first path [14]. EDs based on a simple threshold η which can be determined on the evaluation of the PoED as proposed in [12]. We also assume frequency-selective, slowly varying fading channels. The received signal after elimination of its out-of-band noise through a bandpass filter can be written as

$$r(t) = s(t) + i(t) + n(t) \tag{1}$$

where $s(t)$ is given in [11, eqs. (2) and (3)] as a function of L mutlipath components composed of delays, τ_l's, and path gains, α_l's, for $l = 1, 2, \ldots, L$. In (1) we assume that $i(t)$ represents the NBI and $n(t)$ is the additive white Gaussian noise with one-sided power spectral density, N_0. Additionally, the NBI can be approximated by a single-tone interference [15] with amplitude α_I as

$$i(t) = \sqrt{2I}\alpha_I \cos(2\pi f_I t + \phi_I) \tag{2}$$

where I is the average received power and f_I is the centre frequency of NBI. We also assume that α_I is a random variable (RV) that follows the Nakagami-m distribution given by

$$f_{\alpha_I}(\alpha_I) = \frac{2m^m \alpha_I^{2m-1}}{\Gamma(m)} \mathrm{e}^{-m\alpha_I^2} \tag{3}$$

where m is the Nakagami-m fading parameter and $E\{\alpha_I^2\} = 1$ where $E\{\cdot\}$ denotes expectation. Also, it is assumed that both α_I and φ_I are independent and identically distributed RVs and also φ_I is uniformly distributed over $[0, 2\pi]$.

3 ToA and PoED

3.1 ToA and thresholding

The ToA is equal to the path delay of the direct path, that is, $\tau = \tau_1$ and its estimation is based on $r(t)$. The true delay of the direct path signal τ is contained in the time slot $n_{\mathrm{ToA}} = \lfloor \tau / \mathrm{T_{int}} \rfloor$ (The symbol $\lfloor \cdot \rfloor$ denotes the integer floor function.) where T_{int} is the integration time, for example, the output of the ED is sampled at every T_{int}. So to obtain

doi: 10.1049/iet-wss.2011.0033

the ToA, τ, we need to estimate n_{ToA} which in our case can be effectively estimated by comparing the output of the ED with a predefined fixed threshold η. The selection of an appropriate threshold, η, is critical, since if it is low there will be a high probability to detect signals owing to the presence of noise and interference which is not the first path, and if η is large enough there is a high probability of detecting an erroneous path. So the selection of the appropriate threshold is critical and based on the PoED [12]. The PoED can then be applied to any search-back ToA estimation algorithm and thus the ToA can be easily estimated [14].

3.2 Probability of early detection

The PoED, P_{ED}, and thus the estimation of the ToA of the direct path, is given by [11, eq. (25)]

$$P_{\mathrm{ED}} \simeq \frac{p}{2}(N_{\mathrm{ToA}} - 3) \tag{4}$$

where

$$p = \mathbb{E}_{\mu}\left\{Q_{M/2}\left(\sqrt{2\mu^2}, \sqrt{2\mathrm{TNR}}\right)\right\} \tag{5}$$

μ is an RV given by [11, eq. (21)]

$$\mu = \frac{\alpha_I^2 \mathrm{INR} N_{\mathrm{sym}} T_{\mathrm{int}}}{T_f}[1 + \mathrm{sinc}(2\nu)] = \lambda\gamma_I \tag{6}$$

where $\lambda = \{(\mathrm{INR}N_{\mathrm{sym}}T_{\mathrm{int}})/(T_f)\}[1 + \mathrm{sinc}(2\nu)]$; $\gamma_I = \alpha_I^2$; $\mathrm{INR} \triangleq IT_{\mathrm{s}}/N_0$ is the interference-to-noise ratio; T_{s} is the symbol duration; N_{sym} is the number of symbols of the preamble of each packet for acquisition, synchronisation and ranging; $\mathrm{TNR} \triangleq \eta/N_0$ is the threshold-to-noise ratio (TNR). The parameter N_{ToA} is an integer depending on the ToA τ of the first path and $M = 2WN_tT_{\mathrm{int}}$ is a positive integer where W is the bandwidth of the ideal bandpass zonal filter (BPFZ) where the received signal is incoming first and $N_t = N_{\mathrm{sym}}N_{\mathrm{s}}$ is the number of pulses compose the preamble at the beginning of each packet and N_{s} denotes the number of frames per symbol.

4 Approximation of the PoED

Since α_I follows a Nakagami-m distribution, γ_I is distributed according to a gamma distribution given by

$$f_{\gamma_I}(\gamma_I) = \frac{m^m \gamma_I^{m-1}}{\Gamma(m)} \mathrm{e}^{-m\gamma_I} \tag{7}$$

Using (7) and after a simple transformation of RVs, the distribution of, μ, can be given by

$$f_{\mu}(\mu) = \frac{1}{\lambda} f_{\gamma_I}\left(\frac{\mu}{\lambda}\right) = \frac{m^m}{\lambda^m \Gamma(m)} \mu^{m-1} \mathrm{e}^{-(m\mu/\lambda)} \tag{8}$$

By averaging (5) over (8) the PoED can be evaluated by the following integral

$$\begin{aligned} p &= \int_0^{\infty} Q_N(\sqrt{2\mu^2}, \sqrt{2\mathrm{TNR}}) \frac{m^m}{\lambda^m \Gamma(m)} \mu^{m-1} \mathrm{e}^{-m\mu/\lambda}\, \mathrm{d}\mu \\ &= \frac{m^m}{\lambda^m \Gamma(m)} \int_0^{\infty} \mu^{m-1} \mathrm{e}^{-m\mu/\lambda} Q_N(\sqrt{2\mu^2}, b)\, \mathrm{d}\mu \\ &= \frac{a^m}{\Gamma(m)} \int_0^{\infty} \mu^{m-1} \mathrm{e}^{-a\mu} Q_N(\mu, b)\, \mathrm{d}\mu \end{aligned} \tag{9}$$

where $N = (M/2)$ is a positive integer, $a = (m/\sqrt{2}\lambda)$ and $b = \sqrt{2\mathrm{TNR}}$. To the best of our knowledge, there is not any closed-form solution for the above integral. Therefore our intention is to find an accurate approximate closed-form solution. An accurate approximation for the Marcum Q-function is given in [16, eq. (6)] as

$$Q_N(\mu, b) \simeq \sum_{k=0}^{n} \frac{\Gamma(n+k) n^{1-2k} \mu^{2k} 2^{-k} \Gamma(N+k, (b^2/2))}{\Gamma(k+1)\Gamma(n-k+1)\Gamma(N+k)\mathrm{e}^{(\mu^2/2)}} \tag{10}$$

which is valid for $0 < \mu < 2n$. The above formula for the Marcum Q-function is based on the approximation for the Bessel function given in [17, eq. (5)] and its accuracy increases as n increases. Therefore by applying (10) in (9) we have

$$p \simeq \frac{a^m}{\Gamma(m)} \sum_{k=0}^{n} T_{k,n,N} \int_0^{\infty} \mu^{m+2k-1}\, \mathrm{e}^{-(\mu^2/2)} \mathrm{e}^{-a\mu}\, \mathrm{d}\mu \tag{11}$$

where

$$T_{k,n,N} = \frac{\Gamma(n+k) n^{1-2k} 2^{-k} \Gamma(N+k, (b^2/2))}{\Gamma(k+1)\Gamma(n-k+1)\Gamma(N+k)} \tag{12}$$

The integration in (11) can be evaluated in closed form using [18, eqs. (3.4.62) and (9.240)], [19, eq. (13.1.33)] as

$$p \simeq \frac{a^m}{\Gamma(m)} \sum_{k=0}^{n} T_{k,n,N} 2^{-k-(m/2)} \Gamma(2k+m) U\left(k + \frac{m}{2}, \frac{1}{2}, \frac{a^2}{2}\right) \tag{13}$$

where $U(\cdot, \cdot, \cdot)$ is the Kummer's confluent hypergeometric function of the second kind defined in [19, eq. (13.2.5)]. Now, by substituting (13) in (4) the PEoD can be derived in closed form. More, when the NBI is subject to Rayleigh fading the PoED can be easily extracted by setting $m = 1$.

The derived result can be easily evaluated with any standard commercial mathematical software package and most important is presented in an easily handling finite sum as opposed to semi-infinite nested sums both for Rayleigh- and for Nakagami modelled NBI presented in [11, eq. (28), 12, eq. (38)], respectively.

5 Closed-form bounds for the PoED

It is obvious from (4) that the expectation of the RV p with respect to the fading of the interferer γ_I, that is the expectation of the Marcum Q-function, plays an important role in the evaluation of the PoED. In [20, 21] were presented tight bounds on the generalised Marcum Q-function for $M/2 \in \mathbb{N}$ for all $\alpha \geq 0$, $\beta > 0$ were presented as

$$Q_{M/2-0.5}(\alpha, \beta) < Q_{M/2}(\alpha, \beta)Q_{M/2}(\alpha, \beta) < Q_{M/2+0.5}(\alpha, \beta) \quad (14)$$

or by taking the expectation with respect to μ

$$\mathbb{E}\{Q_{M/2-0.5}(\alpha, \beta) < \mathbb{E}\{Q_{M/2}(\alpha, \beta)\}\mathbb{E}\{Q_{M/2}(\alpha, \beta)\} < \mathbb{E}\{Q_{M/2+0.5}(\alpha, \beta)\} \quad (15)$$

From (14) the order of the Marcum Q-function, $M/2-0.5$ or $M/2+0.5$ is an odd multiple of 0.5 and thus by using [21, eq. (11)] can be evaluated as follows

$$Q_N(\alpha, \beta) = \frac{1}{2}\mathrm{erfc}\left(\frac{\beta+\alpha}{\sqrt{2}}\right) + \frac{1}{2}\mathrm{erfc}\left(\frac{\beta-\alpha}{\sqrt{2}}\right) + \frac{1}{\alpha\sqrt{2\pi}}\sum_{k=0}^{N-1.5}\frac{\beta^{2k}}{2^k}\sum_{q=0}^{k}\frac{(-1)^q(2q)!}{(k-q)!q!}\sum_{i=0}^{2q}\frac{1}{(\alpha\beta)^{2q-i}i!} \times ((-1)^i\,\mathrm{e}^{-((\beta-\alpha)^2/2)} - \mathrm{e}^{-((\beta+\alpha)^2/2)}) \quad (16)$$

where $N = M/2 \pm 0.5$ for the upper and lower bounds of Q-function, respectively.

The bounds of (17) can be evaluated by using (16) and (8) and after some algebraic manipulations can be written as

$$p = \int_0^\infty Q_N(\sqrt{2\mu^2}, \sqrt{2\mathrm{TNR}})\frac{m^m}{\lambda^m\Gamma(m)}\mu^{m-1}\,\mathrm{e}^{-(m\mu/\lambda)}\,\mathrm{d}\mu$$
$$= \frac{m^m}{2\lambda^m\Gamma(m)}\left\{\underbrace{\int_0^\infty \mu^{m-1}\mathrm{e}^{-(m\mu/\lambda)}\mathrm{erfc}(\sqrt{\mathrm{TNR}}+\mu)\,\mathrm{d}\mu}_{I_1} + \underbrace{\int_0^\infty \mu^{m-1}\mathrm{e}^{-(m\mu/\lambda)}\mathrm{erfc}(\sqrt{\mathrm{TNR}}-\mu)\,\mathrm{d}\mu}_{I_2} + \frac{1}{\sqrt{\pi}}\sum_{k=0}^{N-1.5}\mathrm{TNR}^k\sum_{q=0}^{k}\frac{(-1)^q(2q)!}{(k-q)!q!}\sum_{i=0}^{2q}\frac{1}{\sqrt{2\mathrm{TNR}}^{2q-i}i!} \times\left[\frac{(-1)^i}{2^{(2q-i/2)}}\underbrace{\int_0^\infty \mu^{m-2q+i-2}\mathrm{e}^{-(\sqrt{\mathrm{TNR}}-\mu)^2}\mathrm{e}^{-(m\mu/\lambda)}\,\mathrm{d}\mu}_{I_3} - \frac{1}{2^{(2q-i/2)}}\underbrace{\int_0^\infty \mu^{m-2q+i-2}\mathrm{e}^{-(\sqrt{\mathrm{TNR}}+\mu)^2}\mathrm{e}^{-(m\mu/\lambda)}\mathrm{d}\mu}_{I_4}\right]\right\} \quad (17)$$

By assuming that the Nakagami fading parameter m takes only integer values then the integrals I_1 and I_2 can be directly calculated by using [22, eq. (2.8.9.1)] as follows:

$$I_1 = (-1)^{m-1}\frac{\partial^{m-1}}{\partial r^{m-1}}\left[\frac{1}{r}\left(\mathrm{erfc}(\sqrt{\mathrm{TNR}}) - \mathrm{e}^{(r^2+4r\sqrt{\mathrm{TNR}}/4)}\mathrm{erfc}\left(\sqrt{\mathrm{TNR}}+\frac{r}{2}\right)\right)\right] \quad (18a)$$

$$I_2 = (-1)^{m-1}\frac{\partial^{m-1}}{\partial r^{m-1}}\left[\frac{1}{r}\left(\mathrm{erfc}(\sqrt{\mathrm{TNR}}) - \mathrm{e}^{(r^2+4r\sqrt{\mathrm{TNR}}/4)}\mathrm{erfc}\left(\sqrt{\mathrm{TNR}}-\frac{r}{2}\right)\right)\right] \quad (18b)$$

$$I_3 = \frac{1}{2}\mathrm{e}^{-\mathrm{TNR}}\left[\Gamma\left(\frac{-1+i+m-2q}{2}\right) \times {}_1F_1\left(\frac{-1+i+m-2q}{2}, \frac{1}{2}, \frac{(m-2\sqrt{\mathrm{TNR}}\lambda)^2}{4\lambda^2}\right) + \frac{(-m+2\sqrt{\mathrm{TNR}}\lambda)}{\lambda}\Gamma\left(\frac{i+m-2q}{2}\right) \times {}_1F_1\left(\frac{1}{2}(i+m-2q), \frac{3}{2}, \frac{(m-2\sqrt{\mathrm{TNR}}\lambda)^2}{4\lambda^2}\right)\right] \quad (18c)$$

and

$$I_4 = \frac{1}{2}\mathrm{e}^{-\mathrm{TNR}}\left[\Gamma\left(\frac{-1+i+m-2q}{2}\right) \times {}_1F_1\left(\frac{-1+i+m-2q}{2}, \frac{1}{2}, \frac{(m+2\sqrt{\mathrm{TNR}}\lambda)^2}{4\lambda^2}\right) - \frac{(m+2\sqrt{\mathrm{TNR}}\lambda)}{\lambda}\Gamma\left(\frac{i+m-2q}{2}\right) \times {}_1F_1\left(\frac{1}{2}(i+m-2q), \frac{3}{2}, \frac{(m+2\sqrt{\mathrm{TNR}}\lambda)^2}{4\lambda^2}\right)\right] \quad (18d)$$

where $r = m/\lambda$ and ${}_1F_1(\cdot, \cdot;\cdot)$ is the Kummer's confluent hypergeometric function of the first kind defined in [19, eq. (13.1.2)].

When NBI is subjected to Rayleigh fading, that is, $m = 1$, (18a) and (18b) are getting much simpler owing to the fact that the partial derivative with respect to $m-1$ is eliminated.

6 Numerical and simulation results

In this section we derive plots concerning the PoEd. We assume a square root-raised cosine transmitted pulse with roll-off factor 0.6, pulse duration parameter $\tau_\mathrm{p} = 0.8$ ns, and centre frequency $f_0 = 4.0$ GHz. The bandwidth of BPFZ is placed in $W = 1.6$ GHz. The integration time of the ED is assumed to be $T_\mathrm{int} = 2$ ns. The preamble of each packet consists of $N_\mathrm{s} = 4$ pulses per symbol and with a frame duration $T_\mathrm{f} = 128$ ns. The subinterval duration $T = 120$ ns and $T_a = 100$ ns. The considered NBI is modelled as a tone at frequency $f_I = 3.5$ GHz subject to Nakagami-m fading. The results presented are obtained for the IEEE 802.15.4a CM4 channel model characterising non-line-of-sight indoor propagation in large office environment [23]. Also, for the approximative expression given in (13) we use $n = 1000$ summing terms.

doi: 10.1049/iet-wss.2011.0033

In Figs. 2 and 3, we plot the PoEd for different INR values and also for different number of preamble symbols $N_{\text{sym}} = 1$ or $N_{\text{sym}} = 20$ for $m = 2.3$. We also depict the no-interference case for comparison reasons. From Figs. 2 and 3, and given a specific requirement on PoED, (4) can be used to obtain the required threshold, η, through TNR, that is, the ToA estimation. We observe that the PoED is highly affected by the INR and when the number of preamble symbols increase the PoED is also increased.

In Figs. 4 and 5, the lower and upper bounds of the PoED for the case where M is an odd multiple of 0.5 are shown. We therefore select $N_{\text{sym}} = 1$ or $N_{\text{sym}} = 5$, $N_s = 3$, $T_{\text{int}} = 1$ ns and $W = 1.5$ GHz. We observe that the derived lower and upper bounds are very tight and become tighter with the increase in $N_{\text{sym}} = 5$.

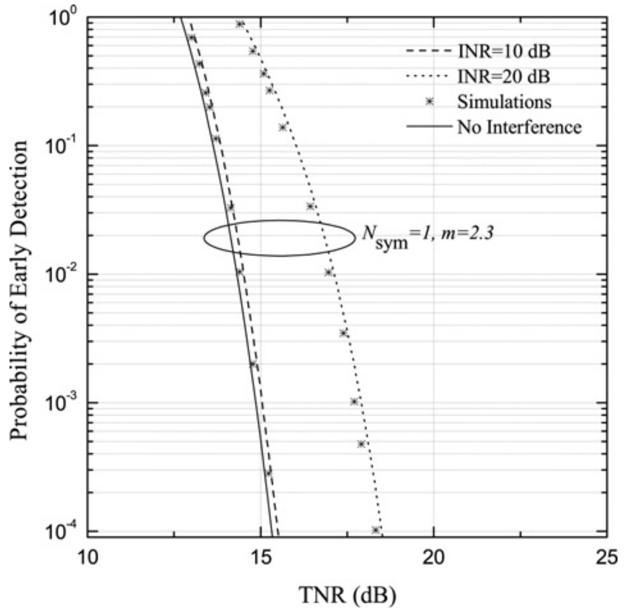

Fig. 2 *PoED in the presence of Nakagami-m NBI for $N_{sym} = 1$*

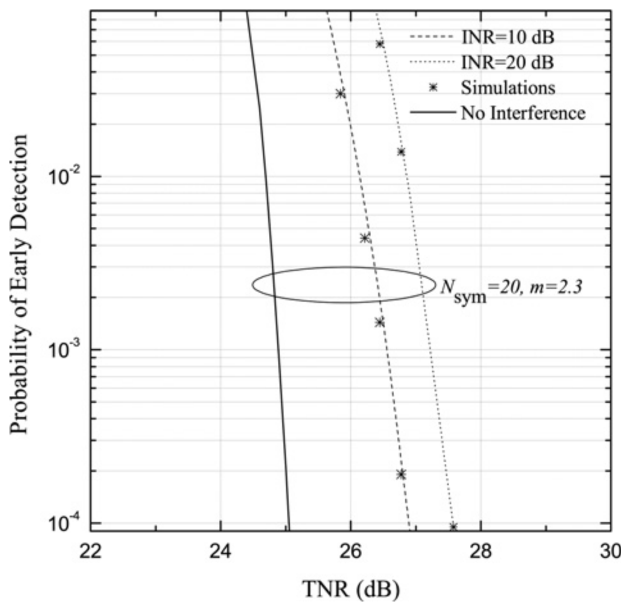

Fig. 3 *PoED in the presence of Nakagami-m NBI for $N_{sym} = 20$*

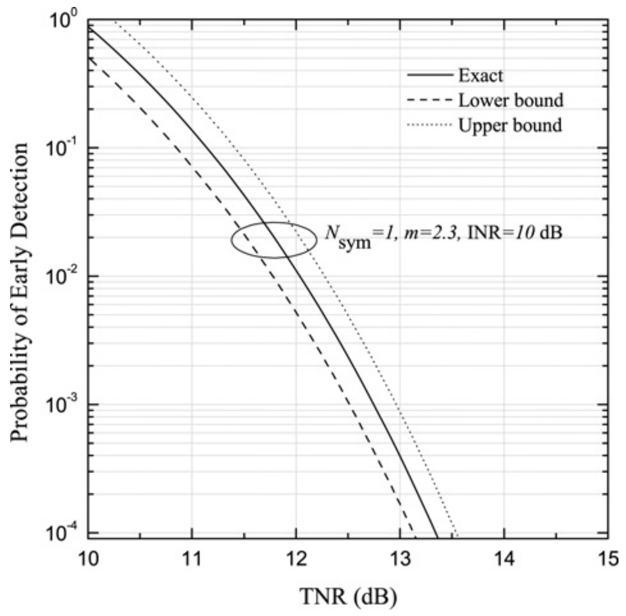

Fig. 4 *Lower and upper bounds for the PoED in the presence of Nakagami-m NBI for $N_{sym} = 1$*

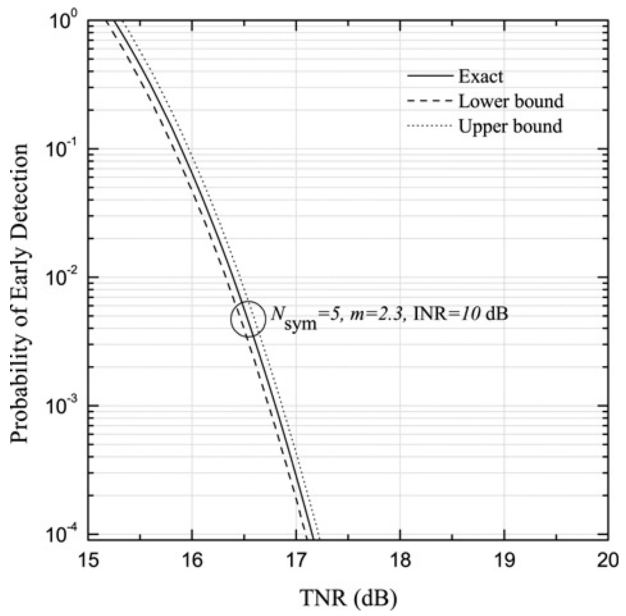

Fig. 5 *Lower and upper bounds for the PoED in the presence of Nakagami-m NBI for $N_{sym} = 5$*

7 Conclusions

The PoED is a significant metric for estimating the ToA of the first path and thus the accurate location of the position of any node in the wireless sensor network. In this work, we have evaluated approximate closed-form expressions for the PoED of the first path of UWB positioning sensor networks when NBI is subject to Nakagami-*m* fading. The derived expressions are given as finite sums of hypergeometric functions as opposed to the semi-infinite sums presented in past works. We have also derived lower and upper closed-form bounds on the PoED. The derived analytical expressions can be a useful mathematical tool for the estimation of the PoED of the first path, that is, the ToA of the first path, and thus locating the position of a wireless sensor node accurately. The overall work does not only enhance the potential of UWB signals for outdoor applications but it can also be an efficient tool to rescue teams saving lives by locating the accurate position of people in disaster areas where a sensor network has been deployed.

8 References

1 Win, M.Z., Scholtz, R.A.: 'On the robustness of ultra-wide bandwidth signals in dense multipath environments', *IEEE Commun. Lett.*, 1998, **2**, (2), pp. 51–53

2 Win, M.Z., Scholtz, R.A.: 'Characterization of ultra-wide bandwidth wireless indoor communications channel: a communication theoretic view', *IEEE J. Sel. Areas Commun.*, 2002, **20**, (9), pp. 1613–1627

3 Oka, A., Lampe, L.: 'Distributed target tracking using signal strength measurements by a wireless sensor network', *IEEE J. Sel. Areas Commun.*, 2010, **28**, (7), pp. 1006–1015

4 Sahinoglu, Z., Gezici, S., Guvenc, I.: 'Ultra-wideband positioning systems theoretical limits, ranging algorithms, and protocols' (Cambridge University Press, 2008)

5 Gezici, S., Tian, Z., Giannakis, G.B., *et al.*: 'Localization via ultra-wideband radios: a look at positioning aspects for future sensor networks', *IEEE Signal Process. Mag.*, 2005, **22**, pp. 70–84

6 Fontana, R.J., Gunderson, S.J.: 'Ultra-wideband precision asset location system'. Proc. IEEE Conf. Ultra Wideband Systems and Technologies (UWBST), Baltimore, Maryland, May 2002, pp. 147–150

7 Falsi, C., Dardari, D., Mucchi, L., Win, M.Z.: 'Time of arrival estimation for UWB localizers in realistic environments', *EURASIP J. Appl. Signal Process. (Special Issue on Wireless Location Technologies and Applications)*, 2006, **2006**, Article ID 32082, pp. 1–13

8 Souza, C.F., Bello, J.: 'UWB signals transmission in outdoor environments for emergency communications'. Eleventh IEEE Int. Conf. Computational Science and Engineering Workshops (CSEWORKSHOPS), 2008

9 Guiliano, R., Mazzenga, F., Petracca, M., Pomposini, R.: 'Wireless opportunistic network based on UWB for preserving environment'. Proc. IEEE Int. Workshops on Enabling Technologies: Infrastructures for Collaborative Enterprises, 2010, pp. 192–196

10 Han, G., Xu, H., Duong, T.Q., Jiang, J., Hara, T.: 'Localization algorithms of wireless sensor networks: a survey', *Spring. Telecommun. Syst. J.*, 2011, accepted

11 Dardari, D., Giorgetti, A., Win, M.Z.: 'Time-of-arrival estimation of UWB signals in the presence of narrowband and wideband interference'. Proc. IEEE Int. Conf. Ultra-Wideband, ICUWB 2007, Singapore, September 2007

12 Dardari, D., Chong, C.-C., Win, M.Z.: 'Threshold-based time-of-arrival estimators in UWB dense multipath channels', *IEEE Trans. Commun.*, 2008, **56**, (8), pp. 1366–1378

13 Dardari, D., Chong, C.-C., Win, M.Z.: 'Analysis of threshold-based TOA estimator in UWB channels'. Proc. European Signal Processing Conf. (EUSIPCO), 2006

14 Guvenc, I., Sahinoglu, Z.: 'Threshold-based TOA estimation for impulse radio UWB systems'. Proc. IEEE Int. Conf. Utra-Wideband (ICU), Zurich, Switzerland, September 2005, pp. 420–425

15 Giorgetti, A., Chiani, M., Win, M.Z.: 'The effect of narrowband interference on wideband wireless communication systems', *IEEE Trans. Commun.*, 2005, **53**, (12), pp. 2139–2149

16 Sofotasios, P.C., Freear, S.: 'Novel expressions for the Marcum and one dimensional *Q*-functions'. Seventh Int. Symp. Wireless Communication Systems (ISWCS), 2010, 19–22 September 2010, pp. 736–740

17 Li, L.-L., Li, F., Gross, F.B.: 'A new polynomial expression for J_m Bessel functions', *Elsevier J. Appl. Math. Comput.*, 2006, **183**, pp. 1220–1225

18 Gradshteyn, I.S., Ryzhik, I.M.: 'Table of integrals, series, and products' (Academic, New York, 1994, 5th edn.)

19 Abramowitz, M., Stegun, I.A.: 'Handbook of mathematical functions with formulas, graphs, and mathematical tables' (Dover, New York, 1972, 9th edn.)

20 Kapinas, V.M., Mihos, S.K., Karagiannidis, G.K.: 'On the monotonicity of the generalized Marcum and Nuttall *Q*-functions', *IEEE Trans. Inf. Theory*, 2009, **55**, (8), pp. 3701–3710

21 Li, R., Kam, P.Y.: 'Computing and bounding the generalized Marcum Q-function via a geometric approach'. Proc. IEEE Int. Symp. Information Theory (ISIT-06), Seattle, WA, USA, June 2006, pp. 1090–1094

22 Prudnikov, A.P., Brychkov, Y.A., Marichev, O.I.: 'Integral and series. Vol. 2: special functions' (Gordon and Breach, New York, 1990)

23 Molisch, A.F., Cassioli, D., Chong, C.-C., *et al.*: 'A comprehensive standardized model for ultrawideband propagation channels', *IEEE Trans. Antennas Propag. (Special Issue on Wireless Communications)*, 2006, **54**, (11), pp. 3151–3166

doi: 10.1049/iet-wss.2011.0033